Geomechanics and Engineering, Vol. 1, No. 1 (2009) 97-112
DOI: http://dx.doi.org/10.12989/gae.2009.1.1.097

Settlement of and load distribution in a granular piled raft

Madhira R. Madhav†

Geoenvironmental Engineering Centre, J.N. Technical University, Hyderabad 500072, India

J. K. Sharma‡

College of Engineering, Kota, India

V. Sivakumar‡†

School of Civil Engineering, Queen's University, Belfast BT7 1QN, Northern Ireland

(Received October 27, 2008, Accepted March 16, 2009)

Abstract. The interactions between a granular pile and raft placed on top are investigated using the continuum approach. The compatibility of vertical and radial displacements along the pile - soil interface and of the vertical displacements along the raft - top of ground interfaces are satisfied. Results show that consideration of radial displacement compatibility does not influence the settlement response of or sharing of the applied load between the granular pile and the raft. The percentage load carried by the granular pile (GP) increases with the increase of its stiffness and decreases with the increase of the relative size of raft. The normal stresses at the raft - soil interface decrease with the increase of stiffness of GP and/or relative length of GP. The influences of GP stiffness and relative length of GP are found to be more for relatively large size of raft. The percentage of load transferred to the base of GP increases with the increase of relative size of raft.

Keywords: granular piles; stone columns; raft; continuum approach; settlement; contact pressures; load sharing.

1. Introduction

Piled rafts are usually employed for the design of foundations on deep deposits of soft soils, to reduce the total and differential settlements of structures. Granular piles may also be used in place of concrete or steel piles because of their several additional advantages. A large number of approaches have been proposed for the analysis of piled rafts. A similar approach may be used for the analysis of granular piled raft foundations. The most conservative of them, which due to its simplicity is often adopted in the design of such foundation systems, considers that the entire building load is carried only by piles, resulting in very expensive solution. Eurocode (1995)

† Professor Emeritus, E-mail: madhavmr@gmail.com
‡ Senior Lecturer
‡† Senior Lecturer, Corresponding author, v.sivakumar@qub.ac.uk

recommends that the raft be assumed to carry a portion of the total load leading to acceptable settlements, while the remaining load is supported by piles.

Various theoretical analyses have been proposed to assess the behaviour of treated ground with granular piles (GP), based on the "Unit Cell" concept (Baumann and Bauer 1974, Aboshi *et al.* 1979, Goughnour and Bayuk 1979, Balaam and Booker 1981, Van Impe and De Beer 1983, Van Impe and Madhav 1994, Priebe 1976 and 1995, Alamgir *et al.* 1996, Poorooshasb and Meyerhof 1997). Interest in the application of granular piles/stone columns in relatively smaller number beneath ordinary footings is increasing in recent times. Muir Wood *et al.* (2000) report a study of footings on large groups of stone columns and identify different deformation mechanisms or patterns such as bulging, shear failure, asymmetric lateral deformation and compression. Watts and Serridge (2000) and Watts *et al.* (2000) report studies on instrumented trial vibro-columns supporting strip foundations at the Bothkenner site and in a variable fill. The former study assesses the consolidation settlement and stress transfer mechanisms through stone columns beneath footings. The latter study reports the effects of installation of GP on the in situ ground conditions. Most recently McKelvey *et al.* (2004) report results on model footing on granular piles of various lengths.

Present study examines two of the mechanisms, viz., punching and elastic compression, identified by Muir Wood *et al.* (2000), in relation to the behaviour respectively of short and long GP. It deals with the computation of mobilized radial or confining stresses generated at the GP-soil interface and their effect on the vertical displacements of the GP and the raft. The overall response in the linear load - settlement response of the GP-raft foundation system in terms of the settlement influence factor, the percentage of load taken by the GP and the normalized contact pressure distribution, are evaluated.

2. Analysis of granular piled raft

Fig. 1 shows a granular piled raft foundation carrying a load, P. The raft is rigid and of diameter, d_r. The granular pile is compressible with modulus of deformation, E_{gp}, Poisson's ratio, ν_{gp}, diameter, d (=2a), and length, L. The surrounding soft soil is characterized by it's modulus of deformation, E_s, and Poisson's ratio, ν_s. Fig. 2(a) depicts the applied force and the mobilized interaction stresses on the raft and the GP with the discretisation scheme used for numerical integration. Fig. 2(b) shows the stress system for the soil with τ and σ_r the interface shear and radial stresses between GP and the in situ soil and p_r - the contact pressures at the raft-soil interface.

Analysis of a rigid raft over an incompressible pile was presented by Poulos (1968). Butterfield and Banerjee (1971b) analyzed of the problem of pile group-pile cap interaction for the stiffness range of concrete and steel piles. Randolph (1983) presented a simple analysis for an incompressible pile with a rigid raft based on average factors for interaction between the raft and the pile. The present analysis uses the continuum approach to determine the stress systems, τ and σ_r, along the soil-granular pile interface and p_r, at the raft - soil interface, which satisfy the compatibility of displacements along the interfaces. For no slip or yield at the GP-soil interface, the GP and the raft displacements are equated to the soil displacements at the corresponding nodes. The stresses and the soil displacements for GP and raft are evaluated based on the interactions of raft on raft, raft on GP, GP on GP and GP on raft. The essential steps of the analysis are the evaluation of: (a) Soil displacements, (b) Granular pile and raft displacements and (c) compatibility displacements. The GP is discretised into, 'n' cylindrical elements as shown in Fig. 2. Each cylindrical element is acted

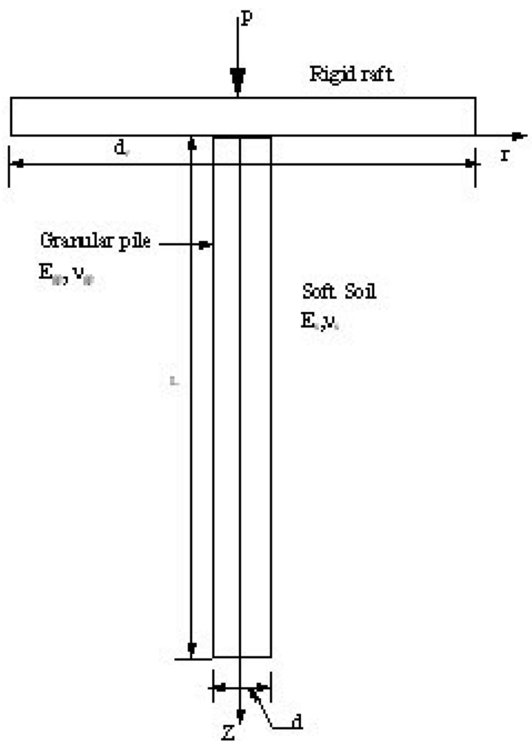

Fig. 1 Definition Sketch

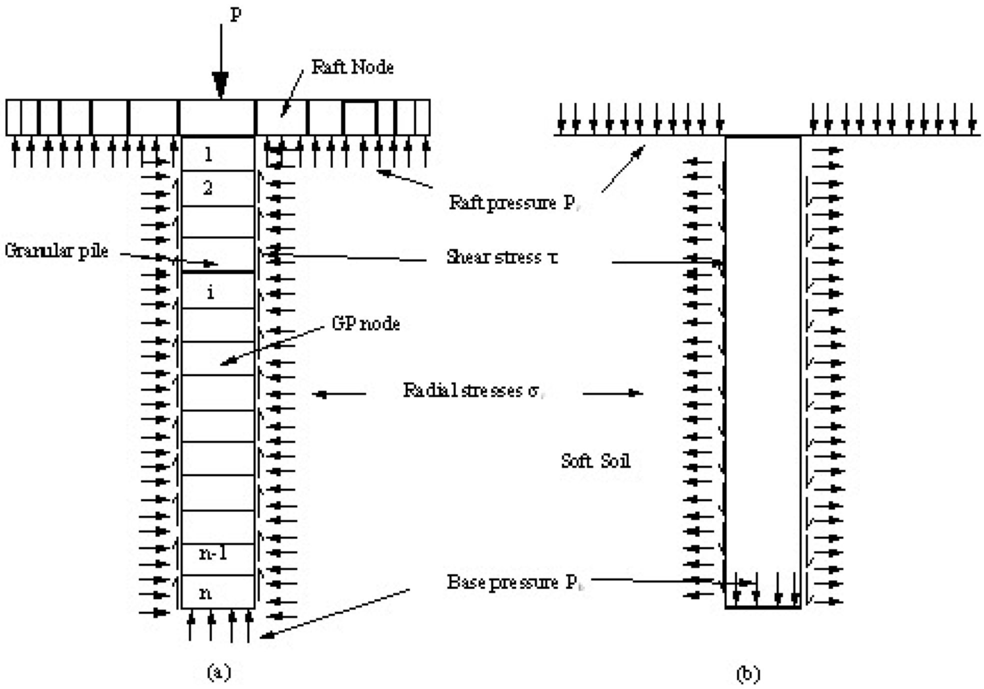

Fig. 2 Forces and Stresses on (a) Raft and Pile and (b) Soil

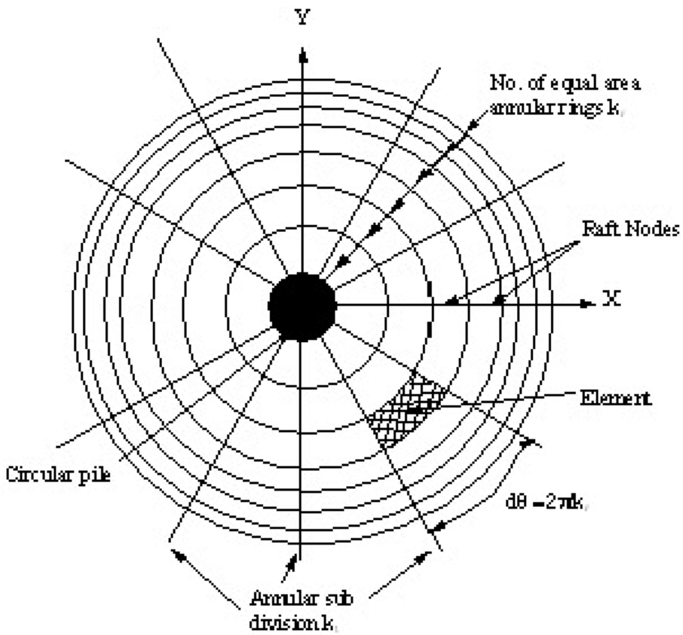

Fig. 3 Discretisation of Raft - Note Equal Areas

upon by shear, τ, and radial, σ_r, stresses at the interface and uniform normal stress, p_b, on the base of GP. It is assumed that the sides of GP are perfectly rough while the base is perfectly smooth. The analysis is presented for a smooth raft. The raft is discretised in to 'k_r' number of annular rings (Fig. 3) of equal areas as division in to annuli of equal width did not give consistent results. It is further subdivided in to 'k_t' number of angular or circumferential sub-divisions.

2.1 Soil displacements

Soil displacements along GP-soil interface and along the raft-soft ground interface are evaluated at the mid-points on the side of each element by integrating Mindlin (1936) and Boussinesq's expressions respectively. The GP is divided in to 'n' elements of length, ΔL ($=L/n$). The stress acting on a typical element, j, is τ_j. The displacement at the centre of an element, i, due to stresses acting on element, j, are obtained by the method described by Poulos and Davis (1980). Integrating numerically, the Mindlin's equation (1936) for a point load in the interior of a semi-infinite elastic continuum over the cylindrical periphery of the element, the displacement, ${}_s\rho_{ij}$, of the soil adjacent to the centre of the ith element due to stress, t_j, acting on the element, j, is obtained as

$$\rho_{s,ij} = \frac{d \cdot I_{s,ij} \cdot \tau_j}{E_s} \tag{1}$$

where $I_{s,ij}$ – is the soil displacement influence coefficient. The total soil displacement, $\rho_{s,i}$, adjacent to node 'i' due to stresses on all the elements of the GPA, is obtained by summing up all the displacements at node 'i', due to stresses on elements j=1 to n, as

$$\rho_{s,i} = \frac{d}{E_S}\sum_{j=1}^{n} I_{S,ij} \cdot \tau_i \tag{2}$$

The soil displacements of all the nodes due to the shear stresses mobilized on it are collated to arrive at

$$\{\rho_s\} = \frac{d \cdot [I_s] \cdot \{\tau\}}{E_s} \tag{3}$$

where $\{\rho_s\}$ and $\{\tau\}$ are respectively the soil displacement and shear stress vectors of size, n, and $[I_s]$ is the soil displacement influence coefficient matrix of size $n \times n$. Similar integrations are carried out for the influences of the normal stresses at the bottom of GP, of radial stresses and the normal stresses at the raft-ground interface on the settlements at various points along GP and raft-ground interfaces.

Details of integration of Mindlin's expressions for horizontal and vertical displacements due to horizontal and vertical point loads within the semi-infinite elastic continuum follow the procedure given in Poulos and Davis (1980) and Sharma (1999). Thus the normalized vertical soil displacements, ρ^{spv}, for nodes along the GP at the midpoint on the periphery of each element and at the centre of the base due to influences of shear, base and radial stresses of GP and raft stresses, p_r, in matrix form are

$$\{\rho^{spv}\} = \left\{\frac{S^{spv}}{d}\right\} = [I^{spvv}]\left\{\frac{\tau}{E_S}\right\} + [I^{sprv}]\left\{\frac{\sigma_r}{E_S}\right\} + [I^{spr_a v}]\left\{\frac{p_r}{E_S}\right\} \tag{4}$$

where $\{S^{spv}\}$ and $\{r^{spv}\}$ are vertical and normalized vertical soil displacement vectors of size, $(n+1)$ each; $[I^{spvv}]$ - is a square matrix of size $(n+1)$ of the coefficients evaluated by integrating Mindlin's equation (vertical displacements due to vertical point load within the semi-infinite elastic medium) for the effect of GP elemental shear stresses and base pressure; $[I^{sprv}]$ - is a matrix of size, $(n+1)\times n$, of the coefficients evaluated by integrating Mindlin's expression (vertical displacements due to horizontal point load within the semi-infinite elastic medium) for the effect of elemental radial stresses on GP; $[I^{spr_a v}]$ - is a matrix of size $(n+1)\times kr$, of the coefficients evaluated by integrating Boussinesq's equation (vertical displacements due to vertical point load at the surface) for the effect of raft stresses on GP nodes; $\{\tau\}$ - is a column vector of size, $(n+1)$, for the shaft stresses and the normal stress on the base, p_b; $\{\sigma_r\}$ - is a column vector of size 'n' for the GP-soil interfacial radial stresses; and $\{p_r\}$- is normal contact pressure vector for raft of size, k_r.

The radial displacements at mid-points of the pile elements and at the raft-ground interface are

$$\{\rho^{spr}\} = \left\{\frac{S^{spr}}{d}\right\} = [I^{spvr}]\left\{\frac{\tau}{E_S}\right\} + [I^{sprr}]\left\{\frac{\sigma_r}{E_S}\right\} + [I^{spr_a r}]\left\{\frac{p_r}{E_S}\right\} \tag{5}$$

where $\{S^{spr}\}$ and $\{\rho^{spr}\}$ are radial and normalized radial soil displacement vectors of size, $(n+1)$ each; $[I^{spvr}]$ - is a matrix of size, $n \times (n+1)$, with the coefficients evaluated by integrating Mindlin's equation (horizontal displacements due to vertical point load within the semi-infinite elastic medium) for the effect of GP elemental shear stresses and base pressure; $[I^{sprr}]$ - is a square matrix of size 'n' of the coefficients evaluated by integrating Mindlin's expression (horizontal displacements due to horizontal point load within the semi-infinite elastic medium) for the effect of interaction radial stresses; and $[I^{spr_a r}]$ - is a matrix of size, $n \times k_r$, of the coefficients evaluated by integrating

Boussinesq's equation (horizontal displacements due to vertical point load at the surface) for the effect of raft stresses.

Soil displacements for raft nodes are evaluated based on the interaction of elemental stresses from raft and GP. The soil displacement equations for raft nodes in matrix form are

$$\{\rho^{sr_a}\} = \left\{\frac{S^{sr_a}}{d}\right\} = [I^{sr_a pv}]\left\{\frac{\tau}{E_S}\right\} + [I^{sr_a pr}]\left\{\frac{\sigma_r}{E_S}\right\} + [I^{sr_a r_a}]\left\{\frac{p_r}{E_S}\right\} \tag{6}$$

where $\{S^{sr_a}\}$ and $\{\rho^{sr_a}\}$ are the soil displacement and normalized soil displacement column vectors of size 'k_r'; $[I^{sr_a pv}]$ - is a matrix of size, $k_r \times (n+1)$, whose coefficients are evaluated for considering the effect of GP elemental stresses on displacements of raft nodes; $[I^{sr_a pr}]$ - is a matrix of size, $k_r \times n$, for the effect of elemental radial stresses on raft displacements; $[I^{sr_a r_a}]$ - is a square matrix of size 'k_r' for the effect of raft stresses on the raft nodes.

2.2 Granular pile and raft displacements

The vertical and radial displacements of GP nodes are obtained as described in Sharma (1999). The vertical GP displacements are expressed as

$$\{\rho^{ppv}\} = \rho_t\{1\} + [D_3]\left\{\frac{\tau}{E_S}\right\} + [C_3]\left\{\frac{\sigma_r}{E_S}\right\} \tag{7}$$

where $\{\rho^{ppv}\}$ is the normalized vertical GP displacement vector of size, $(n+1)$. ρ_t is the normalized top displacement of GP. Details of all the terms of the above equation are given in Sharma (1999). The radial displacements of GP are obtained as

$$\{\rho^{ppr}\} = [G_3]\left\{\frac{\sigma_v}{E_S}\right\} + [F_3]\left\{\frac{\sigma_r}{E_S}\right\} \tag{8}$$

where $\{\rho^{ppr}\}$ are the normalized radial GP displacement vector of size 'n'. Details of all the matrices are available in Sharma (1999).

The raft is considered as rigid and hence displacements of raft nodes are all equal. The displacement of top of the GP (ρ_t) is equal to raft displacement and expressed as

$$\{\rho^{pr_a}\} = \rho_t\{1\} \tag{9}$$

where $\{\rho^{pr_a}\}$ is the raft displacement vector of size 'k_r'.

2.3 Compatibility of displacements

Satisfying the compatibility of displacements for granular pile and the raft, solutions are obtained in terms of shear and radial and raft stresses at the GP-soil and raft-soil interfaces respectively. Applying the compatibility condition for vertical displacements of nodes along GP - soil interface (Eqs. (4) and (7))

$$\{\rho^{spv}\} = \{\rho^{ppv}\} \text{ or}$$

$$[AA_6]\left\{\frac{\tau}{E_S}\right\} + [BB_6]\left\{\frac{\sigma_r}{E_S}\right\} + [I^{spr_a{}^{v}}]\left\{\frac{p_r}{E_S}\right\} = \rho_t\{1\} \tag{10}$$

where $[AA_6] = [I^{spvv}]-[D_3]$, of size $(n+1)\times(n+1)$ and $[BB_6] = [I^{sprv}]-[C_3]$, of size $(n+1)\times n$. Satisfying compatibility of radial displacements along GP-soil interface, i.e., equating Eqs. (5) and (8)

$$\{\rho^{spr}\} = \{\rho^{ppr}\} \text{ or}$$

$$[CC_6]\left\{\frac{\tau}{E_S}\right\} + [DD_6]\left\{\frac{\sigma_r}{E_S}\right\} + [I^{spr_a{}^{r}}]\left\{\frac{p_r}{E_S}\right\} = \{0\} \tag{11}$$

where $[CC_6] = [I^{spvr}]-[G_3]$ is of size $n\times(n+1)$ and $[DD_6] = [I^{sprr}]-[F_3]$ is of size $n\times n$.

For the compatibility of displacements of the points along raft - soil interface (Eqs. (6) and (9))

$$\{\rho^{sr_a}\} = \{\rho^{pr_a}\} \text{ or}$$

$$[I^{sr_a pv}]\left\{\frac{\tau}{E_S}\right\} + [I^{sr_a pr}]\left\{\frac{\sigma_r}{E_S}\right\} + [I^{sr_a{}^{r}a}]\left\{\frac{p_r}{E_S}\right\} = \rho_t\{1\} \tag{12}$$

Eqs. (10), (11) and (12) are solved to obtain the interfacial shear and radial stresses along GP with raft stresses at raft-soil interface. Finally the displacements of raft and GP nodes are obtained.

In case the radial displacement compatibility of GP is ignored (i.e., the effects of radial stresses of GP are not considered in the analysis), Eqs. (10), (11) and (12) get modified to

$$[AA_6]\left\{\frac{\tau}{E_S}\right\} + [I^{spr_a{}^{v}}]\left\{\frac{p_r}{E_S}\right\} = \rho_t\{1\} \tag{13}$$

$$[CC_6]\left\{\frac{\tau}{E_S}\right\} + [I^{spr_a{}^{r}}]\left\{\frac{p_r}{E_S}\right\} = \{0\} \tag{14}$$

$$[I^{sr_a pv}]\left\{\frac{\tau}{E_S}\right\} + [I^{sr_a{}^{r}a}]\left\{\frac{p_r}{E_S}\right\} = \rho_t\{1\} \tag{15}$$

Settlement of GP-raft foundation, S^{pr}, is given as

$$S^{pr} = \frac{P}{E_S d} I^{pr} \tag{16}$$

where I^{pr} is the vertical displacement influence factor for granular piled raft foundation.

The radial displacements, S_r^{pr}, at the GP-soil interface are

$$S_r^{pr} = P/E_s d.I_r^{pr} \tag{17}$$

where I_r^{pr} is radial displacement influence factor. The overall response of GP-raft foundation is evaluated in terms of the vertical displacement influence factor, I^{pr}, the normalized GP-soil interface shear stress, τ, the load ratio, i.e., the percentage of the load taken by the GP to the total load and the normalized contact pressure distribution below the raft. The parameters affecting the overall

Table 1 Comparison of Results for Rigid-Piled Raft ($L/d = 10$, $\nu_s = 0.5$ and $d_r/d = 3$).

K_{gp}	Load on GP (%), $(P_p/P)\times 100$	Ratio of Settlements of Piled Raft to Pile Alone (S^{pr}/S^p)	References
∞	72	0.92	Continuum Approach Poulos (1968)
∞	76	0.96	Approximate Analysis Randolph (1983)
5000	71.2	0.94	Present Study

responses are (i) the geometric ones: the ratio of diameter of the raft to that of GP, i.e., diameter ratio, (d_r/d), and the length to diameter ratio of GP, (L/d), (ii) relative GP-soil stiffness, i.e., $K_{gp} = (E_{gp}/E_s)$, and (iii) Poisson's ratio of the soil, ν_s.

3. Validation

A parametric study was carried out for the following ranges of parameters:

d_r/d = 1-7, L/d = 5-40, K_{gp} = 10-400, ν_{gp} = 0.2-0.3, ν_s = 0.3-0.5. The number of elements 'n' for GP and 'k_r' for raft chosen to satisfy the convergence criterion, vary between 10-50 and 8-20 respectively, depending on the relative length, L/d, of GP and diameter ratio, d_r/d, of the raft. Results obtained by the present analysis (with vertical displacement compatibility of GP) alone compare well with the results of Poulos (1968) and Randolph (1983) for a rigid raft on an incompressible pile (Table 1). The agreement is very close and thus, the proposed analysis validated. Figs. 4 through 15 depict the results from the above analysis. All the results presented below are with the consideration of radial displacement compatibility of GP.

4. Results and discussion

Fig. 4 compares the settlement influence factors, I^{pr}, obtained with and without satisfying radial displacement compatibility at nodes along GP-soil interface, for different relative GP-soil stiffnesses,

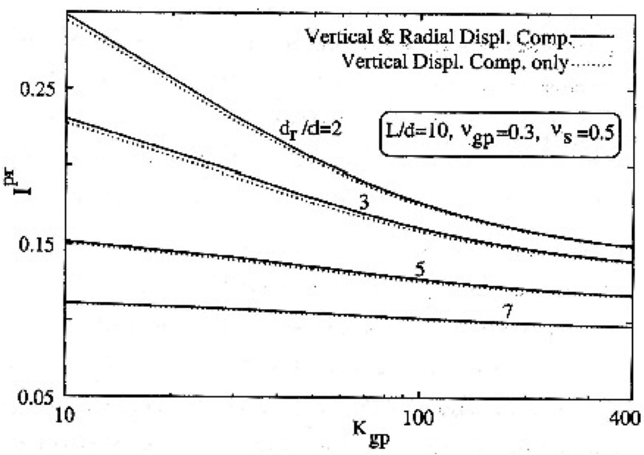

Fig. 4 Comparison of Settlement Influence Coefficients without and with Radial Displacement Compatibility

K_{gp}, and for $L/d = 10$. The differences in the values of I^{pr} obtained from the two analyses are in the range of only 2 to 3% and decrease with increase of relative size of the raft (d_r/d). Thus the consideration of radial displacement compatibility of GP in the analysis does not influence the settlement influence factors. A similar result that the radial displacement compatibility does not affect the settlements of compressible piles was reported by Mattes (1969) for a single compressible pile. The settlement influence factor decreases significantly with the relative stiffness, K_{gp}, of granular pile only in case the relative raft diameter is less than 3. The influence of the granular pile in reducing settlements of the GP-raft system is relatively insignificant in case of large rafts (the area covered by stiff GP is less than 4%) and consequently its influence on settlement influence factor is very small, I^{pr}, decreasing marginally with K_{gp} increasing from 10 to 400.

Variations of settlement factor, I^{pr}, with relative GP-soil stiffness, K_{gp}, for $L/d = 10$ and 20 are depicted in Fig. 5, for different raft to GP diameter ratios. If $d_r/d = 1$, the raft is absent and only the GP is loaded for which the results obtained agree closely with those of Mattes and Poulos (1969) for a single compressible pile alone. The relative GP-soil stiffness ratio has a large effect on I^{pr}, the values of which decrease from 0.26 for K_{gp} = 30 to 0.153 for K_{gp} = 400 for GP alone without raft. The settlement factor, I^{pr}, decreases significantly with the stiffness ratio, K_{gp}, for smaller raft to GP diameter ratios (d_r/d = 2 and 3). Both the compressible pile and the rigid raft influence the overall response of the piled-raft whose settlements decrease with increase in both d_r/d and K_{gp} values. The rate of decrease of I^{pr} with K_{gp} is more for raft resting on longer GP compared to that on shorter one. The values of I^{pr} for $L/d = 10$ and 20 are respectively 0.201 and 0.196 for K_{gp} = 30 and d_r/d = 3. Corresponding values of I^{pr} for K_{gp} = 100 and d_r/d = 3 are 0.160 and 0.140 for L/d = 10 and 20 respectively. However I^{pr} values decrease marginally with K_{gp} for relatively large raft sizes ($d_r/d \geq 5.0$), the influence of stiffness of GP is less significant as discussed above. I^{pr} values decrease from 0.140 for K_{gp} = 30 to 0.118 for K_{gp} = 400 for L/d = 10 and d_r/d = 5.0.

The influence of relative length, L/d, of GP, on the variations of settlement influence factor, I^{pr}, with relative stiffness of GP is depicted in Fig. 6 for d_r/d = 2 and 5. I^{pr} decreases with increasing GP stiffness. This reduction in I^{pr} is significantly more for longer GPs ($L/d \geq 20$). For L/d = 10 and d_r/d=2, I^{pr} reduces from about 0.298 for K_{gp} = 10 to 0.150 for $K = 400$, while for a raft on GP with relative length, $L/d = 25$, the corresponding values of I^{pr} are 0.297 and 0.10 at K_{gp} values of 30 and

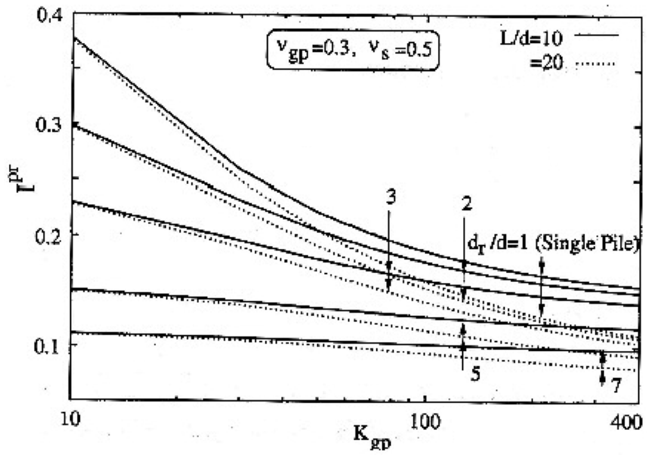

Fig. 5 Effect of Relative Pile Stiffness, K_{gp}, and Raft Size, d_r/d, on Settlement Influence Coefficient, I^{pr}

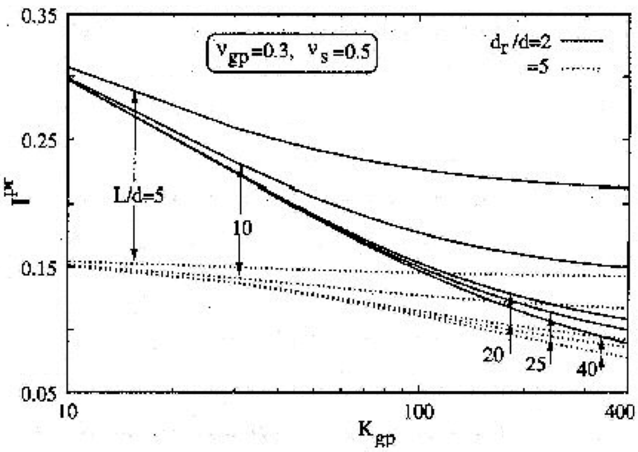

Fig. 6 Effect of Relative Pile Stiffness, K_{gp}, and Pile Length, L/d, on Settlement Influence Coefficient, I^{pr}

400 respectively. Similar results are observed for relatively large size of raft (d_r/d = 5) except that the decrement in I^{pr} with the increase of GP stiffness, K_{gp}, or with relative length, L/d, of GP is less. Most significant conclusion is that the settlement does not reduce significantly with increasing GP length for relatively compressible GP (K_{gp} < 50). Very less to negligibly small loads are transmitted to the bottom of compressible piles (Mattes and Poulos (1969). Consequently increasing the L/d ratio of GP does not contribute settlement reduction for L/d ratios in excess of 15 to 20.

The radial displacement influence factor, I_r^{pr}, decreases with the increase of relative size of raft, d_r/d, except in the lower region of GP where it increases as shown in Fig. 7. The variations of I_r^{pr} with depth normalized with d, i.e., z_1^* (= z/d), are presented for L/d = 10 and 20. The values of I_r^{pr} increase with increase of z_1^* in the range 0 to 5 depending on the relative size of the raft (higher depth for higher values of d_r/d) and then decrease with increasing depths. The maximum radial displacements of GP decrease and shift downward with the increase of d_r/d due to increase in load carried by raft resulting in an increase in the confinement effect of raft. For the same relative sizes

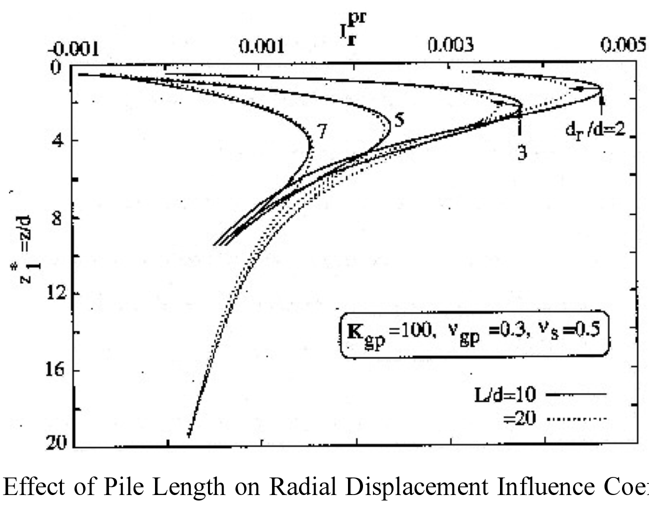

Fig. 7 Effect of Pile Length on Radial Displacement Influence Coefficients

of raft d_r/d, I_r^{pr} values in the region near the top of GP are less for relatively longer GP (L/d = 20) in comparison to those for shorter GP (L/d = 10) except for higher values of d_r/d where the I_r^{pr} is slightly more for longer GP. The differences in the values of I_r^{pr} decrease with increase of d_r/d. The maximum values of I_r^{pr} for d_r/d = 3 observed at a normalized depth of $z_1^* = 2.5$ are about 0.0037 and 0.0034 for L/d = 10 and 20 respectively. In the lower reaches of GP, the radial displacements of GP are very small and almost unaffected by the size of the raft.

The radial displacement influence factor, I_r^{pr}, of GP decreases along its depth with the increase of relative stiffness, K_{gp}, of GP, as shown in Fig. 8. This decrement in I_r^{pr} with K_{gp} is more for relatively smaller size of raft (d_r/d = 2) as compared to the reduction in case of larger one (d_r/d = 5). The maximum value of I_r^{pr} for d_r/d = 2 is observed at a depth of 0.175L and its value decreases from 0.008 for K_{gp} = 30 to 0.0022 for K_{gp} = 1000. The maximum radial displacement for d_r/d = 5 shifts downward to z^* = 0.35.

4.1 Percentage of load carried by granular pile

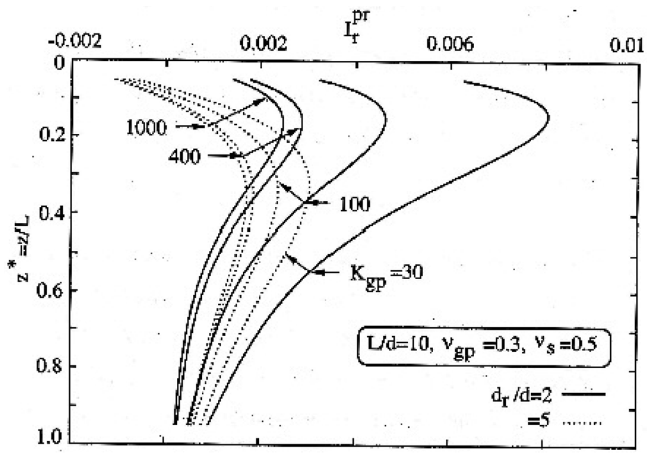

Fig. 8 Effect of Relative Granular Pile Stiffness on Radial Displacement Influence Coefficients

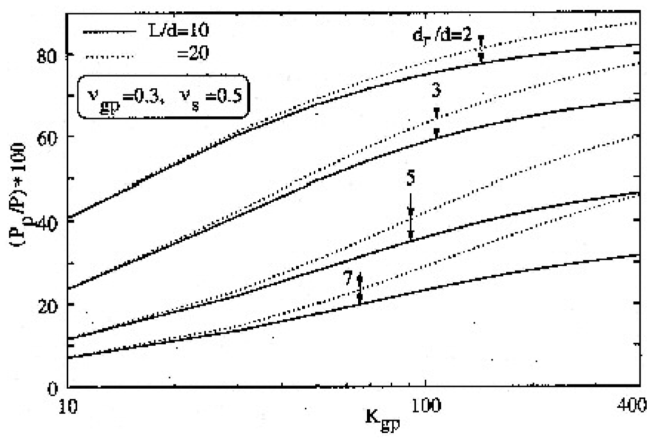

Fig. 9 Effect of Relative Pile Stiffness, K_{gp}, and Raft Size, d_r/d, on Percentage Load Carried by Granular Pile

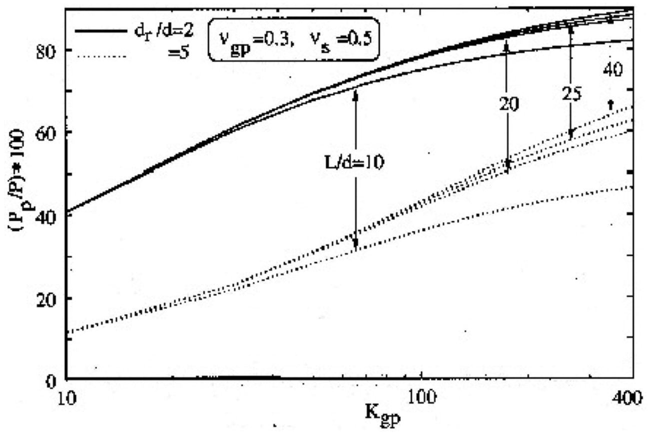

Fig. 10 Effect of Relative Pile Stiffness, K_{gp}, and Pile Length, L/d, on Percentage Load Carried by Granular Pile

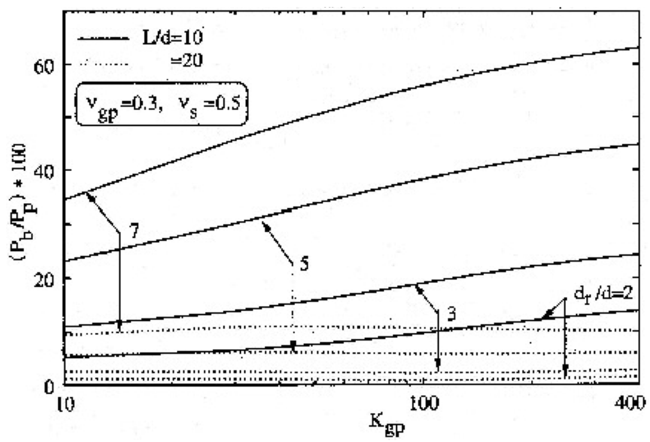

Fig. 11 Effect of Relative Pile Stiffness, K_{gp}, and Raft Size, d_r/d, on Percentage Load Carried to the Granular Pile Base

The influence of the relative GP-soil stiffness as discussed with respect to Fig. 5, can be more clearly noted from the variations of percentage of applied load carried by granular pile, $(P_p/P)\times 100$, with K_{gp}, (Fig. 9), for $L/d = 10$ and 20. For $L/d = 10$ and $d_r/d = 2$, i.e., smaller raft sizes, the percentage load transferred to GP increases from 40% for $K_{gp} = 10$ to 83% for $K_{gp} = 400$. The percentage load carried by the GP decreases with increasing values of d_r/d. For very large raft sizes ($d_r/d = 7$), the percentage GP load is within a narrow range of 8% to 31% for $L/d = 10$ and K_{gp} increasing from 10 to 400. The percentage load carried by relatively longer GP ($L/d = 20$) are more as compared to the loads carried by a shorter one, i.e., $L/d = 10$.

The percentage GP load increases with the increase of relative length of GP, L/d, as shown in Fig. 10. This increment in percentage GP load increases continuously with K_{gp} though with a rate that decreases with increasing K_{gp}. For relative size of raft of $d_r/d = 2$, the increments in percentage GP load with relative length of GP are less as compared to those obtained for $d_r/d = 5$. The percentage GP load for $K_{gp} = 100$ and $d_r/d = 2$ increases from 71 to only 76 for L/d ratio increasing from 10 to

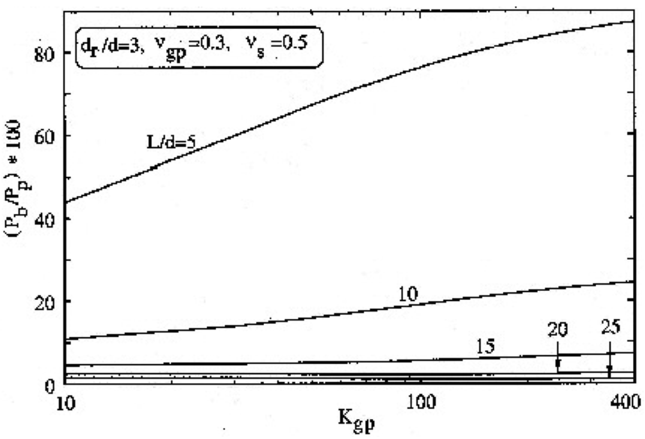

Fig. 12 Effect of Relative Pile Stiffness, K_{gp}, and Pile Length, L/d, on Percentage Load Carried to the Granular Pile Base

40, a four fold increase.

The variation of percentage load transferred to the base of GP, $(P_b/P_p) \times 100$ with K_{gp} is depicted in Fig. 11 along with the influence of relative size of raft. As can be expected, the percentage load transferred to the base of GP increases with the increase of K_{gp}. With the increase of relative size of raft, the percentage load transferred to the base of GP increases because of increase of the interaction effects of raft stresses. For relatively longer GP ($L/d = 20$), the base load is less as compared to that for a shorter one ($L/d = 10$) with similar variation with d_r/d. Fig. 12 shows the effect of relative length of GP on the percentage load transferred to the base of GP. The percentage load transferred to the base for $K_{gp} = 100$ decreases significantly from 19.3 to 0.8 for relative length of GP increasing from 10 to 25.

4.2. Contact pressure distribution

The contact pressure distributions at the raft-soil interface, p_r^* $(= p_r/q$ or $p_r(\pi D^2/4)/P)$, with

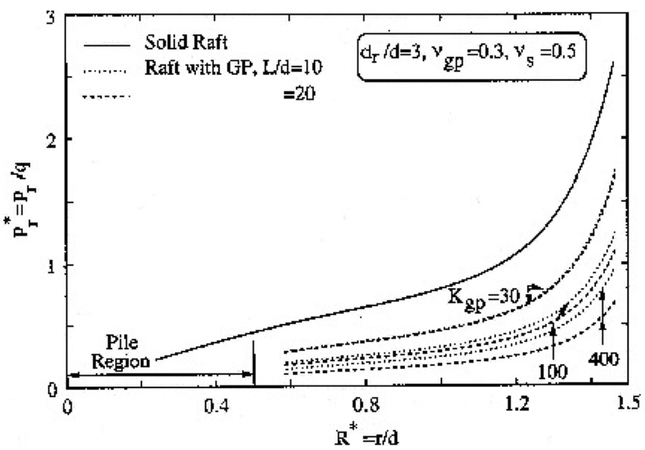

Fig. 13 Contact Pressure Distribution - Effects of Relative Granular Pile Stiffness and Pile Length

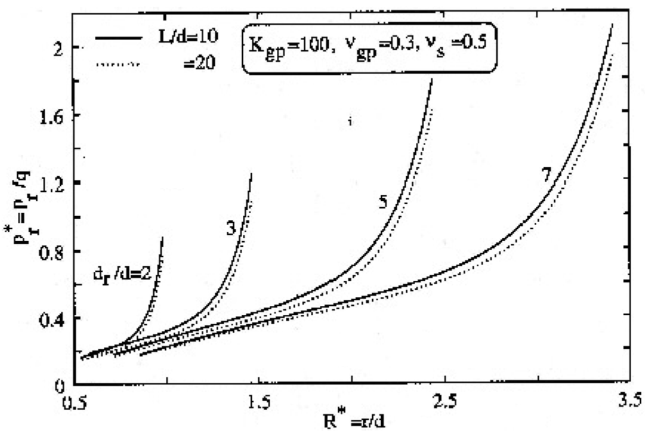

Fig. 14 Contact Pressure Distribution - Effects of Raft Size and Pile Length

normalized distance from the center of raft, $R^* = r/d$ (r is radial distance along raft) can be seen in Fig. 13, for $d_r/d = 3$ and $L/d = 10$ and 20. The patterns are very similar to that of the raft or the footing alone on the surface in that the normal stress beneath a rigid raft increases with distance from the centre and tends to very high values at the edge of the raft. The compressibility of GP has a very significant effect on the magnitude of these stresses. For a typical GP with $L/d = 10$ and $K_{gp} = 30$, the normalized normal stress close to GP is 0.255 and increases to 1.72 at a distance of 1.46 times the GP radius. The corresponding stresses for a relatively stiff GP ($K_{gp} = 400$) are about half of the above values. The normal stresses on raft resting on longer GP ($L/d = 20$) are less in comparison to those on shorter GP ($L/d = 10$) and the differences in the magnitudes increase with the increase of K_{gp}. Fig. 14 depicts the contact pressure distributions for different relative sizes of raft for $K_{gp} = 100$ and $L/d = 10$ and 20. For smaller sizes of raft ($d_r/d = 2$ to 3), a major part of the total load is taken by the GP and as a consequence, contact stresses on the raft are very less. With the increase of relative size of the raft, the magnitudes of normalized normal stresses increase with radial distance. The influence of relative length of GP on normalized normal stresses on raft increases slightly with the increase of its relative size.

5. Conclusions

An analysis of granular piled raft is presented, with and without consideration of radial displacement compatibility of GP. The consideration of radial stresses in the analysis influences the vertical displacement factor of the raft-GP system only marginally. The percentage load carried by GP increases with the increase of its stiffness and decreases with the increase of the relative size of raft. The normal stresses on the raft at the raft - soil interface decrease with the increase of stiffness of GP and/or relative length of GP. The influences of GP stiffness and relative length of GP are found to be more for relatively smaller size of raft. A significant change in the GP behavior due to the presence of raft is to transfer the load to points at depth, i.e., the percentage of load transferred to the base of GP increases with the increase of relative size of the raft but decreases significantly with increase in the relative length of GP.

Acknowledgments

The facilities provided to the first author by Queen's University, Belfast, during the preparation of this paper are gratefully appreciated.

References

Aboshi, H., Ichimoto, E., Enoki, M. and Harada, K. (1979), "The compozer - a method to improve characteristics of soft clays by inclusion of large diameter sand columns", *Proc. Int. Conf. on Soil Reinf.: Reinforced Earth and Other Techniques*, *Paris*: **1**, 211-216.

Alamgir, M., Miura, N., Poorooshasb, H.B. and Madhav, M.R. (1996), "Deformation analysis of soft ground reinforced by columnar inclusions", *Comput. Geotech.*, **18**(4), 267-299.

Balaam, N.P. and Booker, J.R. (1981), "Analysis of rigid raft supported by granular piles", *Int. J. Numer. Anal. Method.*, **5**, 379-403.

Baumann, V. and Bauer, G.E. (1974), "The performance of foundations on various soils stabilized by vibro-compaction method", *Can. Geotech. J.*, **11**, 509-530.

Butterfield, R. and Banerjee, P.K. (1971), "The problem of pile group-pile cap interaction", *Geotech.*, **21**(2), 135-142.

Davis, E.H. and Poulos, H.G. (1972), "The analysis of pile-raft systems", *Aust. Geomech. J.*, **G2**(1), 21-27.

Eurocode (1995), "Design of concrete structures - Part 3: concrete foundations", Prepare for the Commission of European Communities.

Goughnour, R.R. and Bayuk, A.A. (1979), "A field study of long term settlements of loads supported by stone columns in soft ground", *Proc. Int. Conf. on Soil Reinf.: Reinforced Earth and Other Techniques*, *Paris*, **1**, 279-286.

Horikoshi, K. and Randolph, M.F. (1998), "A contribution to optimum design of piled rafts", *Geotech.*, **48**(3), 301-318.

Mattes, N.S. (1969), "The influence of radial displacement compatibility on pile settlement", *Geoteh.*, **19**(2), 157-159.

Mattes, N.S. and Poulus, H.G. (1969), "Settlement of single compressible pile", *J. SM F Div., ASCE*, **95**, 189-207.

Mindlin, R.D. (1936), "Force at a point in the interior of a semi-infinite solid", *J. Appl. Phys.*, **7**(5), 195-202.

Muir Wood, D., Hu, W. and Nash, D.F.T. (2000), "Group effect in stone column foundations: Model tests", *Geotech.*, **50**(6), 689-698.

Poorooshasb, H.B. and Meyerhof, G.G. (1997), "Analysis of behaviour of stone columns and lime columns", *Comput. Geotech.*, **20**(1), 47-70.

Poulos, H.G. (1968), "The influence of rigid pile cap on the settlement behaviour of an axially loaded pile", *C.E. Trans. Inst. Engrs., Australia*, **CE10**(2), 206-208.

Priebe, H. (1976), "Estimating settlement of gravel column consolidated soil", *Die Bautechnik*, **53**, 160-162.

Priebe, H. (1995), The Design of Vibroreplacement, *Ground Engineering*, 31-37.

Randolph, M.F. (1983), "Design of piled raft foundations", *Proc. Int. Symp. On Recent Dev. In Lab. And Field Tests and Anal. Of Geotech. Problems*, *Bangkok*, 525-537.

Sharma, J.K. (1999), "Analysis and settlement of granular pile(s) - single, in group and with raft", *Ph.D. Thesis, I.I.T.*, Kanpur, 408.

Sivakumar, V., McKelvey, D. Graham, J. and Hughes, D. (2004), "Triaxial tests on model sand columns in clay", *Can. Geotech. J.*, **41**, 299-312.

Van Impe, W.F. and De Beer, E. (1983), "Improvement of settlement behaviour of soft layers by means of stone columns", *Proc. 7th EC SMFE*, Helsinki, **1**, 1207-1210.

Van Impe, W.F. and Madhav, M.R. (1992), "Analysis and settlement of dilating stone column reinforced soil", *Osterreichische Ing. und Arch.-Zeitschrift*, **137**, 114-121.

Watts, K.S., Johnson, D., Wood, L.A. and Saad, A. (2000), "An instrumented trial of vibro ground treatment

supporting strip foundations in a variable fill", *Geotech.*, **50**(6), 699-708.
Watts, K.S. and Serridge, C.J. (2000), "A trial vibro bottom-feed stone column treatment in soft clay soil", *4th Int. Conf. on Ground Improvement Geosystems: Grouting, Soil Improvement and Geosystems including Reinforcement*, *Helsinki,* 549-556.

Notation

d	: diameter of the granular pile;
d_r	: diameter of the raft;
E_{gp}	: Modulus of deformation of granular pile;
E_s	: Modulus of deformation of soil;
I	: Settlement influence coefficients;
$K_{gp}=E_{gp}/E_s$	: Modular ratio;
k_r and k_t	: Discretisation in the radial and tangential directions;
L	: Length of the granular pile;
n	: Number of elements the granular pile is discretised into;
P	: Load applied on to the raft;
p_r	: Contact stress at the raft-soil interface;
P_b	: Load transferred to the base of the granular pile;
P_p	: Load carried by the granular pile;
ν_{gp}	: Poisson's ratio of the granular pile;
ν_s	: Poisson's ratio of the soil;
$\rho=S/d$	: Normalised settlement;
σ_r	: Radial stress at the interface between soil and granular pile;
τ	: Shear stress at the interface between soil and granular pile;